10—30 GeV/c ELASTIC SCATTERING OF $\pi^{\pm}+p$, $p+p$, $\tilde{p}+p$ AND $k^{\pm}+p$ OVER THE (t) RANGE 0.0005 TO 1 (GeV/c)^2

K. J. Foley, R. S. Gilmore, R. S. Jones, S. J. Lindenbaum**, W. A. Love, S. Ozaki, E. H. Willen, R. Yamada, L. S. L. Yuan*

Brookhaven National Laboratory
(Presented by S. J. LINDENBAUM)

In this paper, we will report the preliminary results obtained in a series of experiments begun this spring which are still in progress at Brookhaven AGS. The program had two objectives, each of which was met with two partially separate but compatible sets of apparatus.

1. To extend to higher incident momenta our previous measurements [1] in the $|t|$ range 0.2 to 1.0 using the kinematic criteria of coplanarity and the angle between the reciol proton and the forward scattered particle. The apparatus was essentially similar to that previously employed, except for some minor improvements. Fig. 1 shows a schematic of the arrangement.

2. To greatly improve the resolution and precision of our previous [2] small angle scattering experiments so as to cover the Coulomb region, the possible interference region between the real nuclear and real Coulomb amplitude, and finally the nuclear region, all in one high resolution measurement.

One should note that the latter experiment [2] was set up parasitically on the former [1] and, in fact, until introduction of the helium bags, both experiments were run together at the low momenta. Thus, the second set-up was extensively tried out while the first was running.

1. ELASTIC SCATTERING RESULTS FOR THE $t=0.2$ TO 1.0 (GeV/c) RANGE

This experiment essentially used the same arrangement and the digital data handler used in the 1962 experiments. The following are preliminary results, as the experiments are still in progress.

* Work performed under the auspices of the U. S. Atomic Energy Commission.

** Visitor, on the staff of the Rutherford High Energy Laboratory.

The general characteristics of the experiment, including background, various corrections, etc., are similar to those reported in our previous work of this type. The errors shown include all relative errors. The absolute scale calibration is within five percent.

Fig. 2 gives the new results obtained in the 10-25 GeV/c incident momentum range for $\pi^- + p$ which previously extended to only 17 GeV/c. It appears that the lack of appreciable shrinkage observed at the lower momenta [2, 3] persists until 25 GeV/c. The other general characteristics are relatively independent of incident momentum. The $\pi^- + p$ data have been fit by the previously used standard parametric form $d\sigma/dt = e^{a+bt+ct^2}$ and fits with a good χ^2 are obtained.

Fig. 3 gives a one Regge pole fit to (a) all the $\pi^- + p$ data (7-25) GeV/c and (b) 15-25 GeV/c data alone, and fits were obtained in both cases. Although this method of fitting has no a priori simple significance, it is at least a convenient parameterization of the s dependence, namely

$$\frac{d\sigma}{dt} = f(t) \cdot \left(\frac{s}{s_0}\right)^{2\alpha(t)-2}$$

where $\alpha(t) = \alpha + bt$.

For $0.2 \leqslant |t| \leqslant 0.9$ (GeV/c)^2 the results are:

$$\pi^- + p \begin{cases} \text{7-25 GeV/c } \alpha(t) = \\ = (0.961 \pm 0.0312) - (0.052 \pm 0.071)\, t \\ \text{15-25 GeV/c } \alpha(t) = \\ = (0.914 \pm 0.087) - (0.155 \pm 0.200)\, t. \end{cases}$$

Therefore, it is clear that the lack of appreciabte shrinkage as previously shown obtained at the lower momenta persists until 25 GeV/c.

Fig. 4 gives the new results (15-25 GeV/c) obtained for $p + p$ which previously extended only to 19.6 GeV/c. The highly accurate sta-

	NUMBER OF COUNTER ELEMENTS	WIDTH (INCHES)	HEIGHT (INCHES)	THICKNESS (INCHES)
H01	6	.250±.002	1.125	.30
	4	1.125	.250±.002	.30
H02	4	.250±.002	1.125	.30
	4	1.125	.250±.002	.30
H03	4	.250±.002	1.125	.125
	4	1.125	.250±.002	.125
H2	80	.250±.005	6.0	.30
H4	120	.486±.005	13.0	.50
	24	61.0	.486±.005	.50

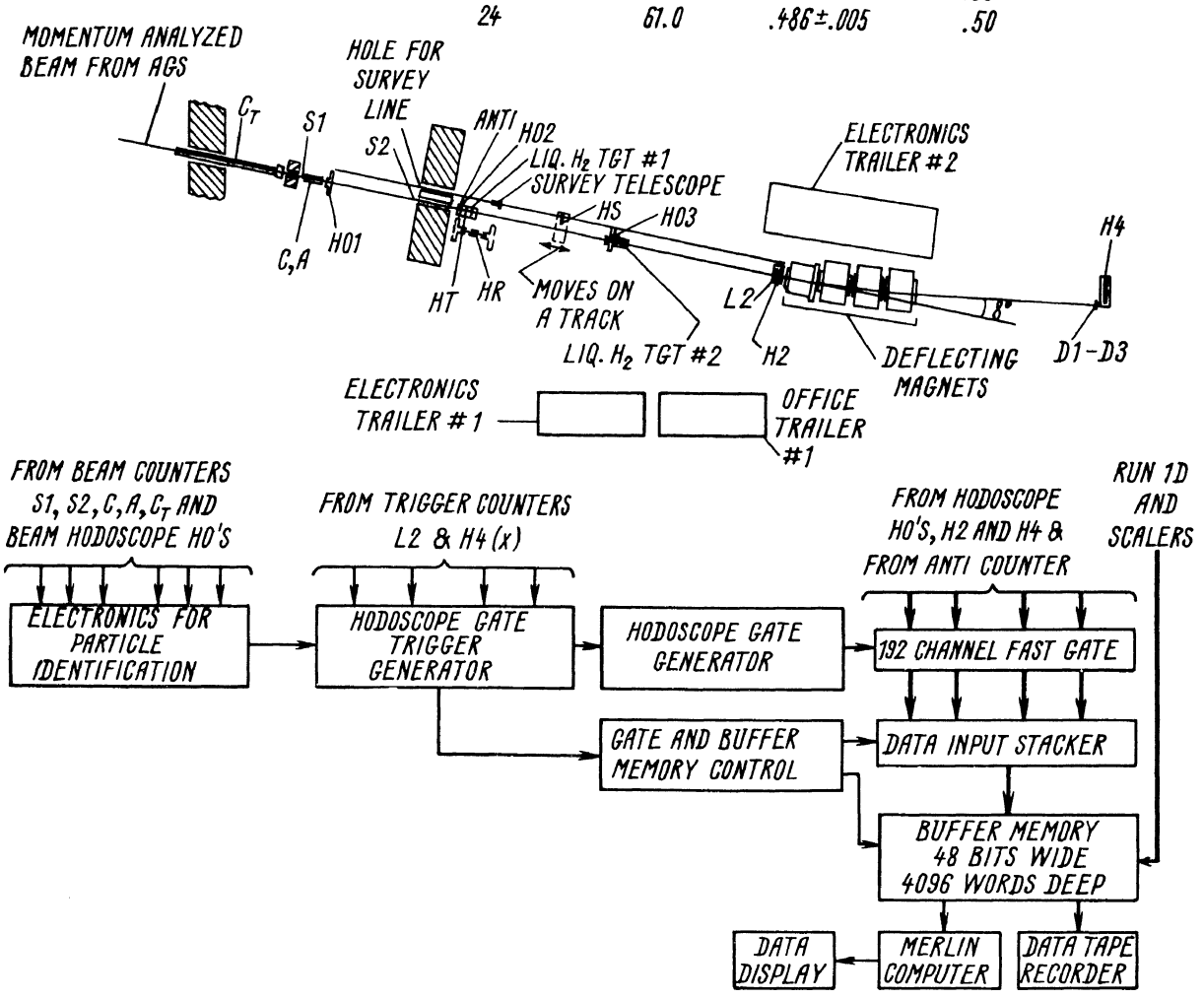

Fig. 1. The experimental arrangement of the elastic scattering measurement in the $|t| \approx 0.2$—1.0 $(\text{GeV/c})^2$ range accompanied by the experimental arrangement of the small angle ($\sim$ 1—25 mr) elastic scattering experiment. Helium bags are used between HO2 and H2 except for small distances around the hodoscopes and hydrogen target. The negative beam production angle is near zero within the range $\pm$ 8 mr. The positive beam production angle is about 65 mr.

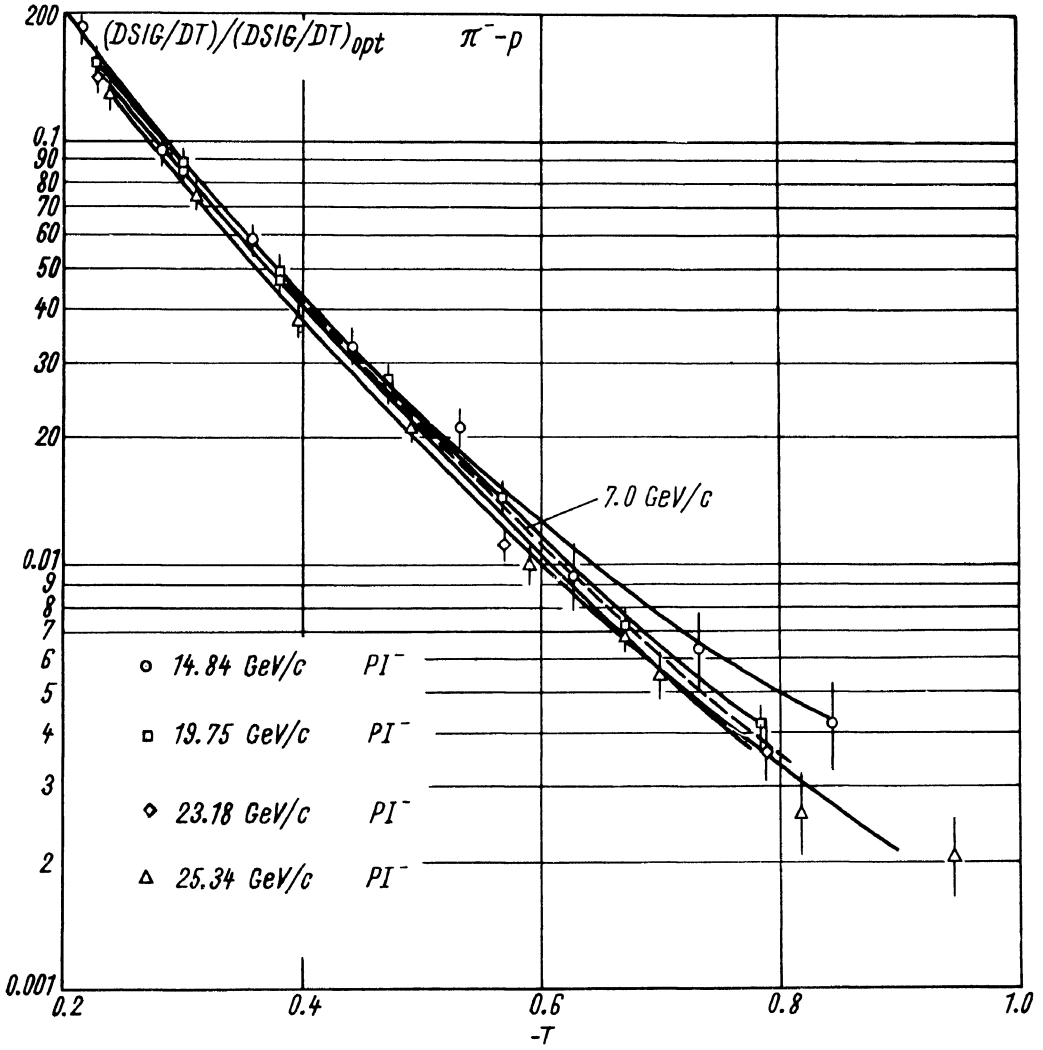

Fig. 2. $d\sigma/dt \Big/ \left(\frac{d\sigma}{dt}\right)$ opt vs. $-t$ for 14.8 to 25.3 $\pi^- + p$ elastic scattering.

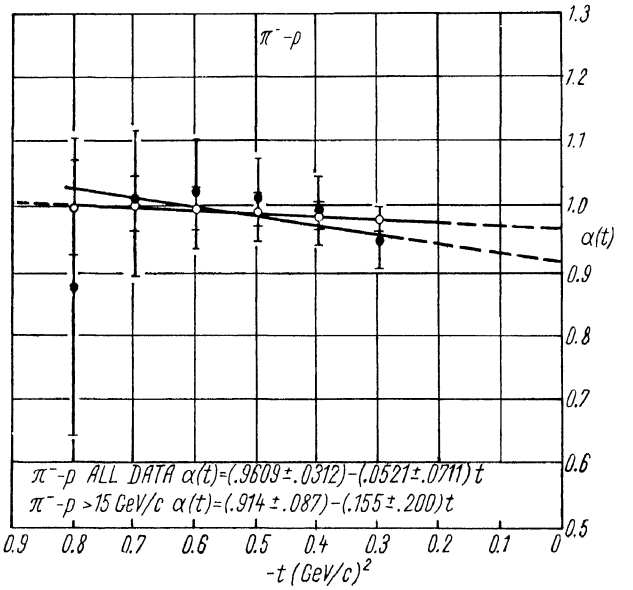

Fig. 3. $\alpha(t)$ vs. $-t$ for a one Regge pole fit.

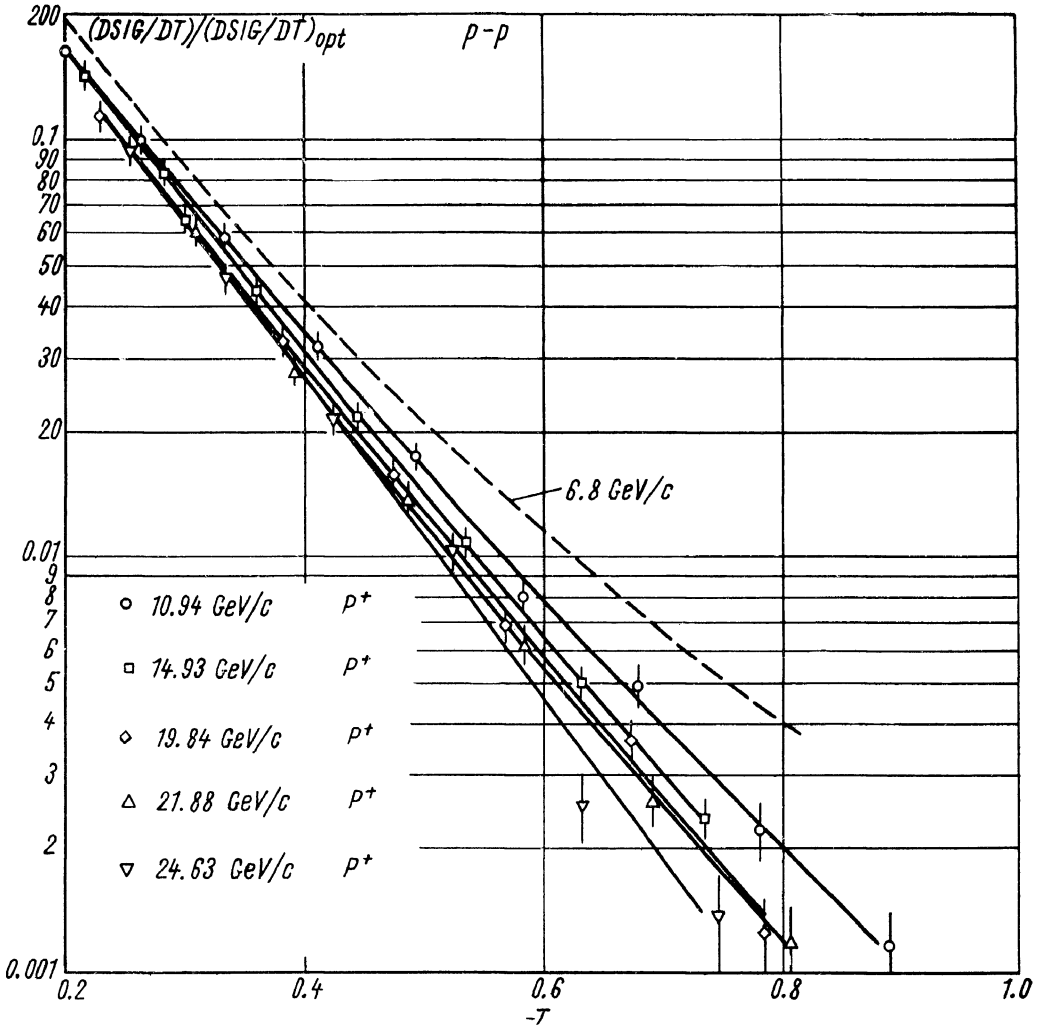

Fig. 4. $d\sigma/dt \Big/ \left(\frac{d\sigma}{dt}\right)$ opt. vs. $-t$ for 15-25 GeV/c $p+p$.

tistics accumulated at 15 GeV/c $p + p$ were used to make an accurate croos-check on the relative calibration of the old (1962) and the present data. It was found that the data from the two runs agree to a fraction of the errors.

One can observe the sizeable shrinkage effects observed at the lower momenta persist at the higher momenta. This is demonstrated quantitatively by Fig. 5 which gives a one Regge pole fit to all the p-p data (7-25 GeV/c) and the 15-25 GeV/c data. The results are:

$$p+p \begin{cases} \text{7-25 GeV/c } \alpha(t) = \\ = (1.05 \pm 0.020) + (0.69 \pm 0.051)\, t \\ \text{15-25 GeV/c } \alpha(t) = \\ = (0.963 \pm 0.080) + (0.378 \pm 0.193)\, t. \end{cases}$$

It is clear then considering the errors there is no convincing evidence for a change in the behavior with varying energy although there may be an indication of a reduction of the shrinkage effect with increasing energy.

Fig. 6 gives the new (12-16 GeV/c) $K^- + p$ results. The old data existed only at 7.2 and 9 GeV/c.

It is clear that the general characteristics of the data are relatively independent of incident momentum and there is no evidence for appreciable shrinkage.

A single Regge pole fit gives:

$$K^- + p \text{ 7-16 GeV/c } \alpha(t) = \\ = (1.106 \pm 0.172) - (0.172 \pm 0.417)\, t$$

indicating a possible but certainly not significant small expansion.

Fig. 7 gives our new results for $\bar{p} + p$.

Fig. 8 gives a one Regge pole fit to all the $\bar{p} + p$ data.

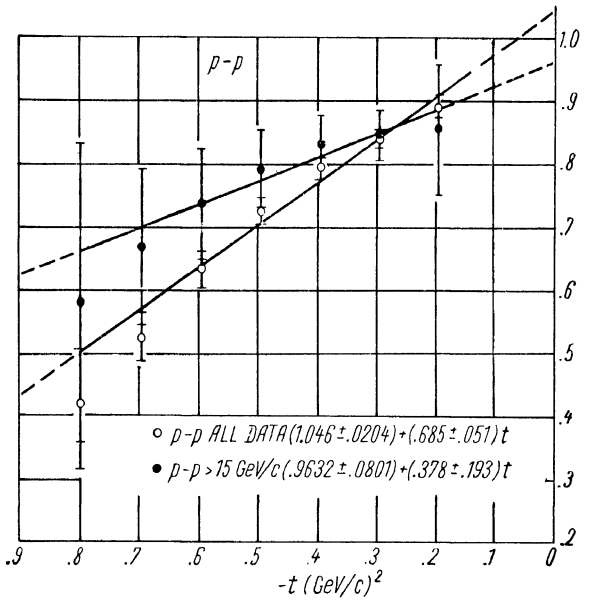

Fig. 5. $\alpha(t)$ vs. $-t$ for $p+p$.

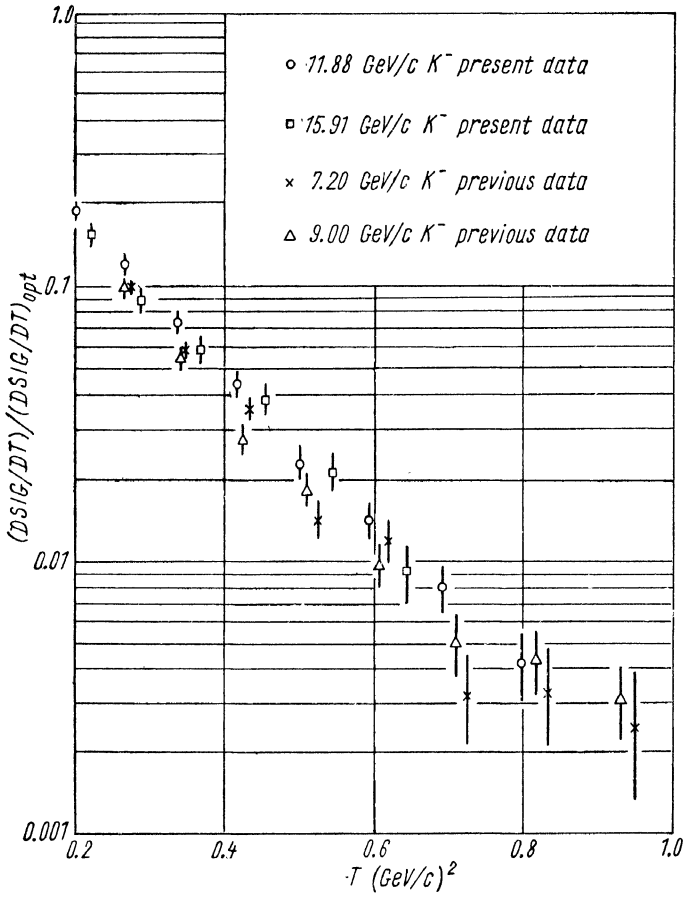

Fig. 6. $d\sigma/dt \Big/ \left(\frac{d\sigma}{dt}\right)$ opt. vs. $-t$ for 7-16 GeV/c $K^- + p$.

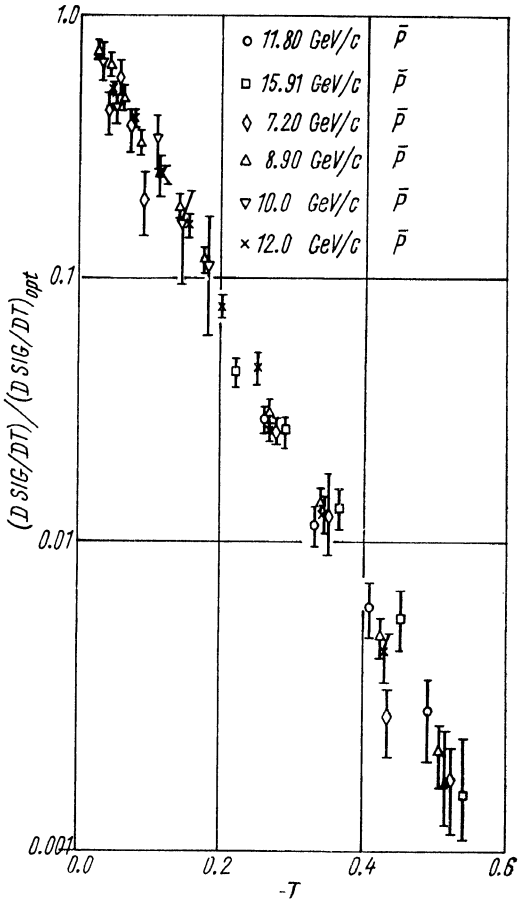

Fig. 7. $d\sigma/dt \Big/ \left(\frac{d\sigma}{dt}\right)$ opt. vs. $-t$ for $\bar{p}+p$.

The result is:

$$\bar{p}+p \text{ 7-16 GeV/c } \alpha(t) =$$
$$= (0.900 \pm 0.084) - (0.915 \pm 0.376)\, t.$$

Therefore, the $\bar{p} + p$ elastic scattering cross-sections indicate expansion with increasing

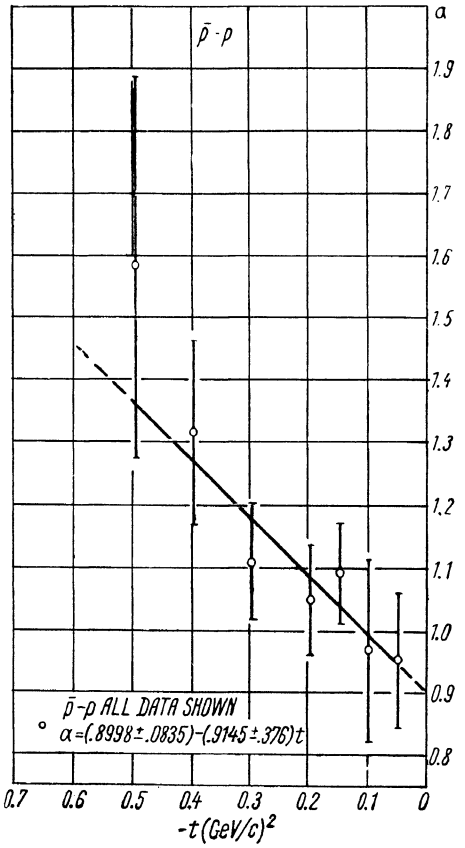

Fig. 8. A single Regge pole fit to all (previous and present) 7-16 GeV/c $p+p$ data.

energy, being somewhat more than two standard deviation difference from no energy dependence.

One should note that the steep slope and consequent large radius associated with the $\bar{p} + p$ interaction has also been observed at lower (~ 4 GeV/c) momenta [4]. A general discussion of particle radii is given in [5] and a scaling law for the fit parameters b and c has been observed by Serber [6].

2. SMALL ANGLE ELASTIC SCATTERING

The incident beam particle is identified by the combination of the differential Čerenkov counter and the threshold Čerenkov counter which is set to detect pions and lighter particles. This counter is used in coincidence for selecting pions and in anticoincidence when selecting heavier particles. 4×4 hodoscopes $\left(\frac{1}{2}''\right.$ wide by $\left.1\frac{1}{8}''\right.$ long) HO2 and HO3 measure the incident particle angle to within ± 0.3 mrad (half width half height). The beam is then scattered in the 18" long H2 target and its scattered position (horizontal) is defined in hodoscope H2 (80 vertical counters $\frac{1}{4}''$ wide by 6" long). The incident particle is then deflected by the bending magnets which follow and its momentum measured to 0.8% by detection in the final hodoscope H4 which contains 120 vertical $\frac{1}{2}''$ wide by 13" high and 24 horizontal counters each 60" long and $\frac{1}{2}''$ wide. Using this set-up the polar scattered angle measured to ± 0.3 mrad in the region of 0-25 milliradians.

The angular distribution of the incident beam and its momentum spectrum can be determined by the combination of HO2, HO3, H2 and H4 when the beam is bent into H4. The beam angular half width is ~ 1 milliradian and the momentum spectrum half width is $\sim 0.8\%$.

Although the incident beam passes right through the angular measuring hodoscope, particles scattered by $\geqslant 2$ mr are selected by trigger counters L2 to avoid filling the data handler with incident beam particle events (which reach intensities 10^5 evenfs/pulse whereas the data handler can handle 1000 events/pulse).

The experiments primarily pursued so far are in the region of 8-15 GeV/c for $p + p$ and $\pi^- + p$. The hydrogen empty background measurement is largest near the beam (first few milliradians) approaching 70%, and drops with increasing angle to only 20-30% at the larger angles. The nature of the background is clearly revealed by the momentum spectrum of the background events which show that 90% of the background events are elastically scattered (by Coulomb and nuclear interactions) particles from the air, scintillator nuclei, etc. Thus this background is a physical cross-section background which is practically independent of beam rates and other small variations and hence can be very reliably subtracted.

In the 8-12 GeV/c incident momentum range we typically record over a million events an hour, of which 90% are elastic scattering. However, the effective statistics on the hydro-

gen cross-section at those $|t|$ where the nuclear amplitude is larger than the Coulomb are greatly reduced from those implied by the above numbers by two effects.

1) The hydrogen cross-section is the difference between the hydrogen in and the hydrogen out counts.

2) A large fraction of events the hydrogen counts are in the Coulomb scattering region.

The first few bins of our angular range are well in the region where Coulomb scattering is much larger than nuclear; however, at the end (high $|t|$ bins) the reverse is true (nuclear Coulomb). Hence we cover the whole range from Coulomb dominated to interference region, to nuclear dominated.

Before discussing the results let us consider the expected form of

1) $d\sigma/dt = A(s, t)^2$

where $A(s, t)$ is the invariant complex scattering amplitude and we have chosen units of $\left[\frac{mb}{(GeV/c^2)}\right]^{1/2}$ for it.

If we make the assumption of a negligible spin dependence of the nuclear interaction, then the expression for the amplitude is:

$$\text{Coulomb} \quad \text{real} \quad \text{imaginary}$$
$$\downarrow \qquad \downarrow \qquad \downarrow$$
2) $$A(s, t) = A(s, t)\, e^{2i\delta} + A(s, t) + iA(s, t)$$

where the relative phase shift between the nuclear and Coulomb amplitudes is $\delta = \frac{e^2}{\hbar v} \ln \frac{1.06}{ka}$ as shown by Bethe.

3) $$A(s, t)^2 = A_c(s, t)^2 + 2A_c(s, t)\,[\cos 2\delta \cdot A_{re}(s, t) + \sin 2\delta \cdot A_{\mathrm{Im}}(s, t)] + A_{re}(s, t)^2 + A_{\mathrm{Im}}(s, t)^2.$$

Experimental evidence for a real amplitude if no spin depende is assumed has been given previously by Kirillova et al [7] for 6.5 and 10 GeV/c $p + p$. See reference [8] for other related papers. These earlier works contained various uncertaintes in the data or analyses.

It is a sufficiently good approximation to use the single photon exchange (Rosenbluth formula) for the Coulomb amplitude which is then real. Form factor effects will not be too important for this analysis, as we are most sensitive to the interference at values of $|t|$ small enough that form factor effects are small (10%). It will be precisely taken into account in the final analysis. For small $|t|$ we can then write the Coulomb amplitude:

4) $$A_c(s, t) = \pm \frac{F}{t};$$

where we take the sign convention «—» for $p + p$ (i. e. repulsion).

Previously [1, 2] we worked at $|t|$ values where the Coulomb amplitude was small compared to the nuclear and found that we could represent the elastic scattering cross-section by

5) $$\frac{d\sigma}{dt} = e^{a+bt+ct^2} |A_{\text{nuclear}}|^2.$$

From the known values of b [10 $(\mathrm{GeV/c})^{-2}$] and c [2 ÷ 3 $(\mathrm{GeV/c})^{-1}$] and recognizing that $|t| \leqslant 0.05$ for the presently reported data, the quadratic term is negligible.

At any one s, let us now assume a real part of the nuclear amplitude which has the same t dependence as the imaginary part and so that the real part has a constant fraction of the imaginary amplitude. The sign of α is taken as negative when the real part has the same sign as a repulsive Coulomb potential. Then with all the above assumptions we find:

6) $$\frac{d\sigma}{dt} \approx \frac{F^2}{t^2} \pm \frac{2\alpha F'}{|t|} e^{\left(\frac{a}{2} + \frac{b}{2} t\right)} + (1 + \alpha^2) e^{a+bt}$$
$$\uparrow \qquad \uparrow \qquad \uparrow$$
$$\text{Coulomb term} \quad \text{interference term} \quad \text{nuclear term}$$

where the «—» sign is for (repulsion) $p + p$, where the «+» sign is for (attraction) $p + p$, F represents the (E. M.) formfactor* and F' takes first order account of both interference terms.

The real Coulomb amplitude interfers with the real nuclear amplitude and the imaginary Coulomb amplitude interfers with the imaginary nuclear amplitude. The imaginary interference is $\leqslant$ 10% of the real interference for the results we obtain and the assumption $F \approx F' \approx F_0$ whose form factor effects are neglected is suitable for preliminary analysis. Due to the optical theorem, a is known from the total cross-section measurements, the only unknowns being α and b. For the case $\alpha = 0$ (no real amplitude) the only true parameter is b.

Fig. 9a is a plot of the measured $\frac{d\sigma}{dt}$ vs. $-t$ for $p + p$ at 8 ÷ 10 GeV/c incident momen-

* Proper account of the structure of both particles must be considered.

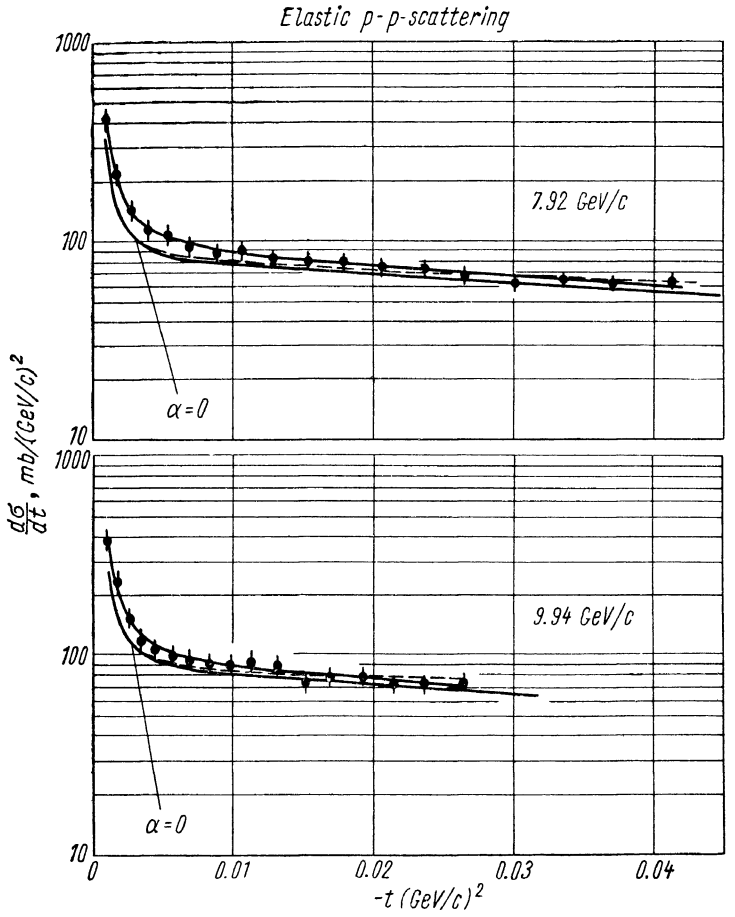

a

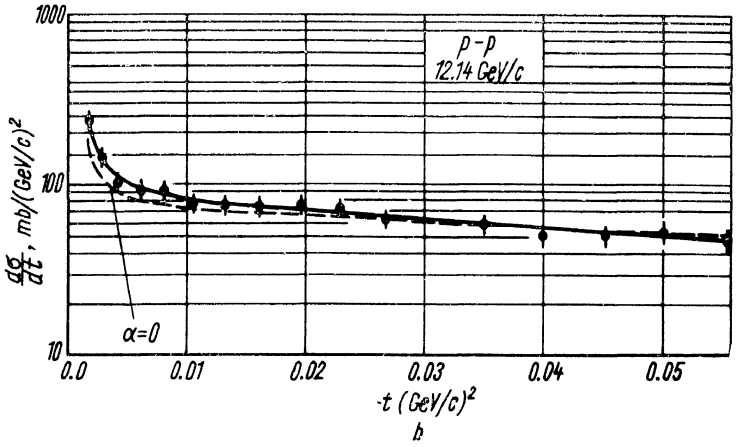

b

Fig. 9. (*a*) 7.92 and 9.94 GeV/c small angle $p + p$ scattering $d\sigma/dt$ vs. $-t$. The theoretical curves were calculated from eq. (6). (See text for details). 9. (*b*) 12.4 GeV/c small angle $p + p$ scattering.

tum. Fig. 9b a plot of the 12.14 GeV/c $p + p$ data. The error flags include estimates of the various systematic errors in relative values as well as the statistical errors.

For comparison a least squares fit of eq. (6) is shown (solid line); a fit with $\alpha = 0$ (dashed line); and the computed no real part curve with $\alpha = 0$ and the same b value as the best fit (also solid line).

The $\alpha = 0$ fits had a χ^2 of 167 for 15 degrees of freedom, which is an entirely unacceptable fit.

There are two major uncertainties in this analysis:

(1) Errors on the coefficient a due to the error on the total cross-section.

(2) Errors on the absolute efficiency of the measurement of $d\sigma/dt$.

These uncertainties must be included, since we find they shift the value of α. During the fit with the appropriate variations of the systematically uncertain quantities we find the following results:

7.92 GeV/c incident momentum p-p

$$\alpha = -0.253 \pm 0.02 \begin{vmatrix} +0.088 \\ -0.088 \end{vmatrix}$$

$$12.14 \text{ GeV/c} \quad \alpha = -0.254 \pm 0{,}02 \begin{vmatrix} +0.10 \\ -0.12 \end{vmatrix}$$

9.94 GeV/c incident momentum p-p

$$\alpha = -0.260 \pm 0.02 \begin{vmatrix} +0.090 \\ -0.088 \end{vmatrix}$$

For the 7.92 GeV/c p-p the $\chi^2 = 30$ for 15 degrees of freedom, which is still an acceptable fit. For the 9.94 GeV/c p-p the $\chi^2 = 15$ for 16 degrees of freedom, which is a good fit.

Let us now explain the (new) notation introduced above for the 8 GeV/c case as an example. The mean value of within the range of values obtained by varying the efficiency total cross-section and other errors over their possible range of values is stated. The superscript error on the right is the upper and lower extreme shift in this mean value as the range of uncertainty of efficiency and total cross-section is swept out in the fit. The error next to α is the typical fit error on any one value of α determined when the efficiency and total cross-section are fixed and assumed known. Hence the prediction for 8 GeV/c p-p is that α lies in the range -0.165 to -0.34 and that the statistical fluctuation outside this range have a standard deviation value of 0.02. Therefore, we see that according to the assumption of this analysis we have good evidence for a real part of the amplitude in $p + p$ of the order of 15 to 35% of the imaginary amplitude in the momentum range of 8-12 GeV/c. These results yield a smaller than the mean values of Kirillova et al [7] and are compatible with the same t dependence for the real and imaginary part, although Kirillova et al. stated their results were not compatible with the same t dependence. The new results of this group reported at the conference and our results are in excellent agreement. Of course, our weakest assumption is that there is no spin dependence of nuclear forces. If we relax this assumption and allow different slopes and amplitudes of the triplet and singlet states we may be able to explain the data without the necessity of inventing a real part of the nuclear scattering amplitude. Such an analysis has been made* and it indeed is the case that one can also explain the experimental results with a much steeper singlet than triplet imaginary part with about the same α.

Another point worth looking into is if we still assume no spin dependence but allow the real part to have a different slope than the imaginary part, what happens? The proper equation would be:

$$d\sigma/dt = \frac{F^2}{t^2} - \frac{2\alpha F'}{t} e^{\frac{a}{2} + \frac{b_r t}{2}} + \alpha^2 e^{a + b_r t} + e^{a + b_{im} t}$$

The results are that the real part has a much steeper t dependence.

Therefore, we conclude the following:

(1) Unless there is a sizeable spin dependence, there is a real part of the 8—10 GeV/c $p + p$ scattering amplitude at low $|t|$ [$\leqslant 0.05$ (GeV/c)^2] which has an amplitude:

$$\sim 0.26 \pm 0.02 \begin{vmatrix} +0.09 \\ -0.09 \end{vmatrix}$$

times the imaginary amplitude if it has the same slope.

---

* We are still neglecting spin flip amplitudes. This is reasonable for small t when considering the (σn) terms since they go to zero as $t \to 0$. However, as discussed by Goldberger and Watson (in Collision Theory Sect. 71., published by Wiley, 1964), there is a $(\sigma_1 \sigma_2)$ spin flip amplitude term which does not vanish as $t \to 0$.

However, it is likely that if a real part exist and there is no sizeable spin dependence the slope of the real part ($|t|$ dependence) is larger than the imaginary. The sign of the real part is the same as the p-p Coulomb amplitude, and hence the real part would correspond to a repulsive interaction. Although the magnitude of the effects we find are smaller. For

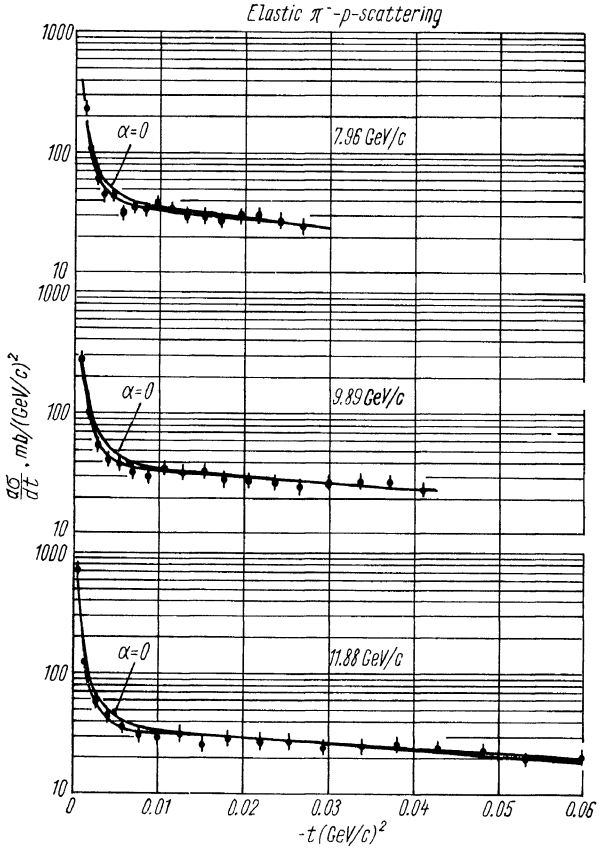

Fig. 10. Small angle $\pi^- + p$ scattering $d\sigma/dt$ vs. $-t$. The theoretical curves were calculated from eq. (6). (See text for details.)

references to the previous work which gave various degrees of evidence for a real part, see [8, 9].

Now let us consider the $\pi^- + p$ case.

Here since the pion is pinless we can describe the elastic scattering by only one spin state amplitude. Although there is a non spin flip and a spin flip amplitude, the latter goes to zero as t goes to 0 since it is of the form $(\boldsymbol{\sigma} \cdot \boldsymbol{n})$ and hence it is reasonable to assume that it is small at small t and neglect it. Therefore, if we assume the real part of the nuclear scattering amplitude has the same slope (i. e t dependence) as the imaginary part and α is the ratio of the amplitudes obtain eq. (6) again.

The $\pi^- + p$ results at 8-12 GeV/c incident pion momenta are shown in Fig. 10, where the $\alpha = 0$ and best fit predictions of eq.(6) are shown for comparison along with the calculated solution for $\alpha = 0$ using the same b as the best fit.

It is clear that the $\alpha = 0$ curve represents a very poor fit. The least squares fits to eq. (6) were made and the efficiency, total cross-section errors, contamination errors, etc. were varied over their ranges.

We obtain at 7.96 Gev/c $\chi^2 = 15.3$ for 15 degrees of freedom

$$\alpha = -0.21 \pm 0.04 \begin{vmatrix} +0.13 \\ -0.14 \end{vmatrix}$$

at 9.89 Gev/c $\chi^2 = 17.9$ for 16 of degrees freedom

$$\alpha = -0.23 \pm 0.0 \begin{matrix} +0.13 \\ -0.13 \end{matrix}$$

and at 11.88 Gev/c $\chi^2 = 19.5$ for 17 degrees of freedom

$$\alpha = -0.27 \pm 0.05 \begin{vmatrix} +0.13 \\ -0.14 \end{vmatrix}$$

Therefore, we conclude that there is good evidence for a real part of the nuclear scatte-

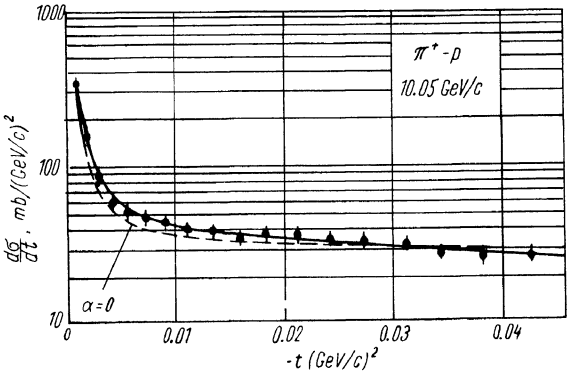

Fig. 11. 10.05 GeV/c $\pi^+ + p$ small angle scattering.

ring amplitude for 8-12 GeV/c $\pi^- + p$ and it is of opposite sign to the Coulomb amplitude which means the real nuclear part is of the same sign as that in the $p + p$ case (a repulsive interaction*).

* As mentioned previously spin flip amplitudes have been neglected in this analysis, since these amplitudes go as $\sigma n \to 0$ as $t \to 0$.

Fig. 11 shows the results obtained for 10.05 GeV/c π^+/p. Here we again see constructive interference and the volue of α is

$$\alpha = -0.33 \pm 0.025 \begin{vmatrix} +0.11 \\ -0.11 \end{vmatrix}$$

Therefore, we conclude that in $\pi^- + p$ (8 ÷ 12 GeV/c) and in $\pi^+ + p$ ($\sim$ 10 GeV/c) these is convincing evidence for a sizable real amplitude which is of the some sign (repulsive) and similar magnetude. In the 8-12 GeV/c $p + p$ case we cannot draw a similar conclusion due to the possible explanation of the observer effects is being due to the spin dependence. However since the observed effects are in $p + p$ are similar to those in $\pi^{\pm} + p$ the simplest interpretation is that they are also due to a real amplitude of the some sign and similar magnitude. Finally one should note that a comparison of these results and other experiments reported at the conference with each other and the dispersion relations is of considerable interest in both checking the dispersion relations and discussion about asymptotic b avior. Since such a comparison is made in the rapporteur's report, pion-nucleon interactions above 1 GeV by S. Lindenbaum the reader is refered to it.

REFERENCES

1. Foley K. J. et al. Phys. Rev. Lett., **10**, 376 (1963); **10**, 543 (1963).
2. Foley K. J. et al. Phys. Rev. Lett., **11**, 425 (1963); **11**, 503 (1963).
3. Caldwell et al. Proceedings of the Sienna International Conference on Elementary Particles, **VI**, 601 (1963).
4. (a) Czyzewski et al. Proceedings of the Sienna International Conference on Elementary Particles, **VI**, 252 (1963).
   (b) Baltay et al. Reports presented at Stanford Conference on Nuclear Structure, July, 1963.
5. Lindenbaum S. J. Proceedings of the 1963 Standford International Conference on Nuclear Structure.
6. Serber R. Phys. Rev. Lett., **13**, 32 (1964).
7. Bethe H. Ann. Der Phys., F. **3**, 190 (1958).
8. Kirillova et al. Proceedings of the Sienna International Conference on Elementary Particles, **VI**, 593 (1963) and JETP **18**, 866 (1964).
9. (a) Eggstain and Kellner, Proceedings of the Sienna International Conference on Elementary Particles, **VI**, 598 (1963);
   (b) Bull V. A. and Garbutt D. A. Phys. Rev., **130**, 1182 (1960);
   (c) Preston et al. Phys. Rev., **118**, 579 (1960);
   (d) See Reference [2].